## ISSN: 2349-5162 | ESTD Year: 2014 | Monthly Issue JOURNAL OF EMERGING TECHNOLOGIES AND



INNOVATIVE RESEARCH (JETIR)

An International Scholarly Open Access, Peer-reviewed, Refereed Journal

# In Silico Elucidation of the Inhibitory Mechanism of Chickpea Peptide CaNCR63 against Staphylococcus aureus Sortase A

<sup>1</sup>Rajendra Choure, <sup>2</sup>Nidhin Suresh, <sup>3</sup>Yash Pawar, <sup>4</sup>Sarang Lobhi, <sup>5</sup>Rupendra Jadhav

<sup>1</sup> Assistant Professor, <sup>2</sup>Masters student, <sup>3</sup>Masters student, <sup>4</sup>Masters student, <sup>5</sup>Professor, <sup>1</sup>Department of Microbiology, <sup>1</sup>Institute of Science, Dr. Homi Bhabha State University, Mumbai, India

Abstract: The rising threat of antimicrobial resistance (AMR) in pathogens like methicillin- resistant Staphylococcus aureus (MRSA) demands novel therapeutic strategies. Anti-virulence therapy, which targets virulence factors instead of cell viability, offers a promising approach to mitigate the selective pressure for resistance. Sortase A (SrtA), a membrane-associated transpeptidase that anchors key virulence factors to the cell wall of S. aureus, is a primary anti-virulence target. This study employs an in silico approach, integrating molecular docking and 150 ns molecular dynamics (MD) simulations, to evaluate the chickpea peptide CaNCR63 as a potential inhibitor against S. aureus SrtA (PDB ID: 1T2W). Docking analysis predicted a favorable binding orientation for CaNCR63 within the catalytic groove of SrtA. However, subsequent 150 ns MD simulations, performed to validate this pose, revealed that the complex was transient and ultimately unstable. The peptide failed to remain anchored and dissociated from the active site after approximately 110 ns. A detailed analysis of the trajectory provided a clear molecular explanation for this instability. Despite forming geometrically favorable, near-linear hydrogen bonds with the active site, the peptide's high internal flexibility and likely unfavorable desolvation energetics were sufficient to overcome these interactions, leading to dissociation. These findings establish that while CaNCR63 is a promising hit from docking, it is an unstable, transient binder, not a potent inhibitor. This study highlights the critical importance of MD simulations in validating static docking hits and provides a robust molecular framework for the rational optimization of the CaNCR63 scaffold for the development of novel anti-virulence therapeutics.

IndexTerms - Antimicrobial Resistance (AMR), Staphylococcus aureus, Sortase A (SrtA), Anti-virulence, Peptide Inhibitor, Molecular Dynamics Simulation, Molecular Docking

#### I. INTRODUCTION

Antimicrobial resistance (AMR) has emerged as one of the most significant global health threat of the 21st century, posing a severe threat to public health and the effectiveness of current medical treatments (Ho et al. 2025; Zrelovs et al. 2021; Ha, Yi, and Paek 2020; Basu, Khanra, and Pal 2025). The World Health Organization (WHO) has consistently emphasized that the rise of AMR could reverse decades of progress in infection control and modern medicine. Staphylococcus aureus, particularly methicillin-resistant S. aureus (MRSA), is a major pathogen at the center of this crisis, due to its clinical prevalence and pathogenic diversity (Ho et al. 2025; Tran et al. 2025; Ha, Yi, and Paek 2020; Y. Chen et al. 2024; Balachandran 2017). It is responsible for causing broad spectrum of infections, ranging from superficial skin lesions to life-threatening conditions such as endocarditis, pneumonia, septicemia, etc. The increasing failure of traditional antibiotics due to widespread resistance necessitates the urgent development of novel therapeutic strategies (Zrelovs et al. 2021; Ha, Yi, and Paek 2020; Basu, Khanra, and Pal 2025).

One promising alternative is anti-virulence therapy, which targets bacterial pathogenicity factors rather than essential survival processes (Abujubara et al. 2023; Zrelovs et al. 2021; Ha, Yi, and Paek 2020; Basu, Khanra, and Pal 2025; Tran et al. 2025). This approach is hypothesized to exert a lower selective pressure, thereby reducing the likelihood of resistance emergence (Zrelovs et al. 2021; Abujubara et al. 2023; Y. Chen et al. 2024; Basu, Khanra, and Pal 2025). In Gram-positive bacteria, Sortase A (SrtA) has emerged as a potential anti-virulence target due to its key role in surface protein anchoring and pathogenesis(Zrelovs et al. 2021; Ha, Yi, and Paek 2020; Abujubara et al. 2023; Basu, Khanra, and Pal 2025; Tran et al. 2025; Balachandran 2017; Y. Chen et al. 2024; Maghsoodlou, Fozouni, and Salehnia Sammak 2022; Asmara, Hernawan, and Nuzlia 2024). SrtA anchors a suite of microbial surface components recognizing adhesive matrix molecules (MSCRAMMs), such as Protein A and fibrinogen-binding proteins, to the peptidoglycan cell wall (Zrelovs et al. 2021; Ha, Yi, and Paek 2020; Basu, Khanra, and Pal 2025; Abujubara et al. 2023; Apostolos et al. 2022; Balachandran 2017). This anchoring is crucial for

bacterial adhesion to host tissues, biofilm establishment and immune evasion (Tran et al. 2025; Y. Chen et al. 2024; Zrelovs et al. 2021; Ha, Yi, and Paek 2020; Basu, Khanra, and Pal 2025; Balachandran 2017; Maghsoodlou, Fozouni, and Salehnia Sammak 2022).

The catalytic mechanism of SrtA involves recognition of the conserved LPXTG motif at the C-terminus of its protein substrates. The thiol group of the catalytic residue Cys184 performs a nucleophilic attack on the threonine residue of this motif, forming a thioacyl intermediate (Abujubara et al. 2023; Ha, Yi, and Paek 2020; Basu, Khanra, and Pal 2025; Apostolos et al. 2022). This reaction is facilitated by the conserved catalytic triad, which also includes His120 and Arg197 (Naik et al. 2006; Tran et al. 2025; Y. Chen et al. 2024; Abujubara et al. 2023; Basu, Khanra, and Pal 2025; Asmara, Hernawan, and Nuzlia 2024). Given its pivotal role in virulence and its non-essentiality for bacterial growth, SrtA is an favorable target for the design of novel inhibitors (Zrelovs et al. 2021; Ha, Yi, and Paek 2020; Balachandran 2017; Y. Chen et al. 2024). Previous studies have identified various small-molecule SrtA inhibitors, including natural compounds like flavonoids (e.g., luteolin, myricetin, plantamajoside), fatty acids and also some synthetic compounds (Tran et al. 2025; Y. Chen et al. 2024; Maghsoodlou, Fozouni, and Salehnia Sammak 2022; Asmara,

Hernawan, and Nuzlia 2024; Basu, Khanra, and Pal 2025). However, the development of clinically viable drugs remains a challenge. Peptide-based inhibitors, derived from the natural LPXTG substrate, offer a promising alternative due to their potential for high specificity and rational design (Abujubara et al. 2023).

Beyond substrate mimetics, naturally occurring plant peptides represent another vast reservoir of potential inhibitors, known to be sources of novel antimicrobial molecules active against human pathogens. Our investigation focused on CaNCR63, a nodulespecific cysteine-rich (NCR) peptide originally identified in chickpea. Given that CaNCR63 has demonstrated inhibitory activity against other bacterial targets(Lima et al. 2022), we hypothesized that it might function as a broad-spectrum inhibitor capable of engaging multiple virulence factors. To test this hypothesis against a critical Gram-positive target, we sought to evaluate CaNCR63's potential to bind and inhibit S. aureus Sortase A.

In this study, we adopted a comprehensive *in silico* strategy combining molecular docking and a 150 ns molecular dynamics (MD) simulation to evaluate ability of CaNCR63 as a peptide inhibitor, CaNCR63, targeting S. aureus SrtA (PDB ID: 1T2W). Our aim was to elucidate the binding conformation of CaNCR63, assess the stability of the peptide-enzyme complex, and characterize its molecular interactions within the SrtA catalytic site. Our analysis found that while molecular docking predicted a favorable binding pose, the subsequent 150 ns MD simulation revealed the binding to be transient. The peptide maintained its interactions for approximately 110 ns before dissociating from the active site. These findings underscore the critical importance of dynamic simulations in assessing the stability of static docking poses and establish CaNCR63 as a promising scaffold for further rational optimization against S. aureus.

#### II. MATERIALS AND METHODS

#### Peptide Sequence and 3D Structure Modeling

The primary amino acid sequence of the chickpea peptide CaNCR63, "KMICKTRVDCKKYRCPRSKIKDCVKGYCRCVRKK," was obtained from the published chickpea NCR catalog Montiel et al. 2017. As no experimental structure is available, an initial threedimensional model of CaNCR63 was generated using the SWISS-MODEL homology modeling server Waterhouse et al. 2018. The resulting structure was then prepared using UCSF Chimera Pettersen et al. 2004. Hydrogen atoms were added and the structure was energy-minimized to resolve any unfavorable geometries prior to docking.

#### **Receptor Structure Preparation**

The high-resolution crystal structure of S. aureus Sortase A (SrtA) was retrieved from the Protein Data Bank (PDB ID: 1T2W) Zong et al. 2004. The structure was prepared for docking using The PyMOL Molecular Graphics System Schrödinger 2015. All crystallographic water molecules and co-solvents were removed and hydrogen atoms were added to the protein structure.

#### Molecular Docking of CaNCR63 to Sortase A

Molecular docking was performed to predict the binding orientation and affinity of CaNCR63 within the SrtA active site using Dockit pipeline Gasiunas 2020. During the docking protocol, both the SrtA receptor and CaNCR63 peptide were treated as a rigid bodies. The docking search space was defined by a grid box to ensure comprehensive sampling of the substrate-binding groove. The docking run was performed with an exhaustiveness of 16 and the resulting poses were ranked by their binding affinity scores. The topranked conformation, which demonstrated plausible interactions with the catalytic triad, was selected for subsequent molecular dynamics simulations.

#### **System Setup for Molecular Dynamics**

Two distinct systems were constructed for simulation using the CHARMM-GUI web server Lee et al. 2016: (1) the apo-SrtA enzyme and (2) the SrtA-CaNCR63 complex derived from the best-ranked docking pose. Each system was placed in an orthorhombic periodic box and solvated with TIP3P water molecules, ensuring a minimum distance of 15 °A between the protein and the box boundaries. To mimic physiological conditions essential for SrtA activity, each system was neutralized and ions were added to achieve a Ca2+/Cl- salt concentration of 15 mM. The CHARMM36m force field was assigned for both the protein and the peptide.

#### **Molecular Dynamics Simulations**

All molecular dynamics (MD) simulations were performed with GROMACS using a leap-frog integrator and a 2 fs time step Abraham et al. 2022. Long-range electrostatic interactions were treated using the Particle Mesh Ewald (PME) method with a real-space cutoff of 1.2 nm. Van der Waals interactions were truncated at 1.2 nm and bond lengths involving hydrogen atoms were constrained

using the LINCS algorithm. The temperature was maintained at 310 K using the V-rescale thermostat and the pressure was controlled semi-isotropically at 1 bar using the Parrinello-Rahman barostat.

Prior to production runs, each system underwent energy minimization using the steepest descent algorithm for 5000 steps, followed by a two-stage equilibration protocol. The systems were first equilibrated in an NVT ensemble for 1 ns, followed by a 5 ns NPT equilibration, with position restraints on heavy atoms gradually released. Finally, unrestrained production MD simulations were carried out for 150 ns for each system. Trajectory coordinates were saved every 100 ps for subsequent analysis.

#### **Trajectory Analysis and Binding Energetics**

Simulation trajectories were post-processed to remove periodicity and center the complex. Structural stability was assessed by calculating the backbone root-mean-square deviation (RMSD), while flexibility profiles were quantified using per-residue root-meansquare fluctuations (RMSF). The overall compactness was evaluated using the radius of gyration (Rg). Interfacial stability was characterized by monitoring the number of hydrogen bonds, the minimum distance and the total number of atomic contacts (within 4 A°) between SrtA and CaNCR63. To quantify the thermodynamic favorability of binding, the binding free energy (ΔGbind) was calculated using the Molecular Mechanics/Poisson-Boltzmann Surface Area (MM/PBSA) method as implemented in the g mmpbsa tool. For this calculation, 100 snapshots were extracted at regular intervals from the stable portion of the trajectory (from 50 ns to 100 ns), prior to the dissociation event.

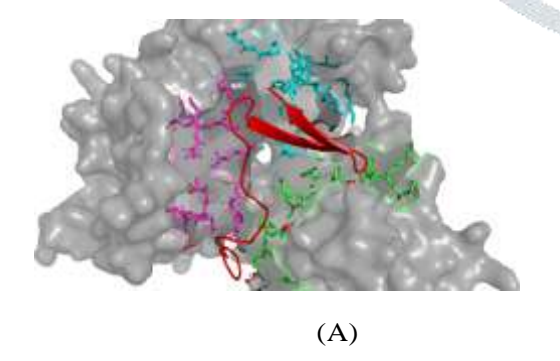
#### III. RESULTS

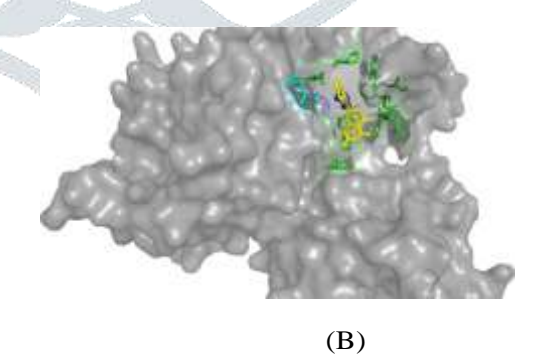
#### Virtual Screening and Molecular Docking

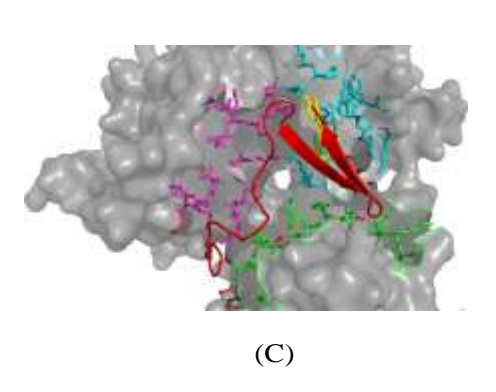
To identify novel peptide-based inhibitors for Staphylococcus aureus Sortase A (SrtA), we performed molecular docking studies using the crystal structure of SrtA (PDB ID: 1T2W) (Zong et al. 2004). SrtA is a validated antivirulence target; as a transpeptidase, it is essential for anchoring virulence factors containing the LPXTG motif to the bacterial cell wall, a key step in S. aureus pathogenesis (Basu, Khanra, and Pal 2025; Zrelovs et al. 2021; Ha, Yi, and Paek 2020; Tran et al. 2025; Balachandran 2017). The lead peptide CaNCR63 was docked into the enzyme's catalytic active site to evaluate its inhibitory potential.

The predicted binding pose of CaNCR63 (Figure 1A) places it securely within the substrate-binding groove. A comparative visualization confirms that CaNCR63 occupies the same active site pocket as the known reference flavonoid inhibitor, luteolin (Figures 1B and 1C). This catalytic site is formed by a groove leading to the conserved catalytic triad, His120, Cys184, and Arg197 (Abujubara et al. 2023; Asmara, Hernawan, and Nuzlia 2024; Naik et al. 2006). The binding energy funnel plot (Figure 1D), generated from an ensemble of docking conformations, confirms that the identified pose represents a distinct and deep energetic minimum, validating it as the most probable and stable binding conformation.

A detailed analysis of the intermolecular interactions reveals the molecular basis for this binding. CaNCR63 forms an extensive network of hydrogen bonds and hydrophobic interactions with catalytically important residues. These interactions are summarized in Table 1. Notably, our peptide shares several critical interaction points with the reference inhibitor luteolin, including interactions with Pro94, Asn98, the catalytic His120, Phe122, Asp124, Asp186, Tyr187, Trp194, and Lys206. The formation of these extensive interactions, particularly with residues involved in natural substrate recognition and catalysis (Naik et al. 2006; Abujubara et al. 2023; Tran et al. 2025), supports the hypothesis that CaNCR63 may act as a potential competitive inhibitor by occupying the same LPXTG substrate-binding pocket.







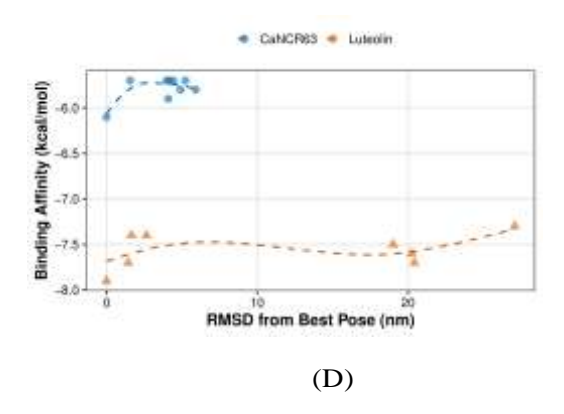


Figure 1: Molecular interactions of Sortase A (grey surface) with inhibitors. (A) The peptide CaNCR63 (red cartoon) binding to a similar region. (B) The known inhibitor Luteolin (yellow sticks) bound within the active site, with catalytic residue B-His120 highlighted in blue. (C) Overlay view illustrating the common binding pocket. (D) Docking funnel plot comparing binding affinities of luteolin (orange triangles,  $\sim -7.5 \ kcal/mol$ ) and CaNCR63 (blue circles,  $\sim -6.0 \ kcal/mol$ ).

#### **Global Stability Assessment**

To validate the binding pose and assess the stability of the SrtA-CaNCR63 complex predicted by docking, we performed a 150 ns molecular dynamics (MD) simulation. A parallel simulation of the unbound (apo) SrtA was also performed as a control. The global stability was assessed by calculating the Root Mean Square Deviation (RMSD) of the protein backbone ( $C\alpha$  atoms) (Figure 2A) and the CaNCR63 ligand (Figure 4A). The simulation revealed a transient binding event. The control 'SortaseA apo' simulation (red line, Figure 2A) remained comapritively stable for 150 ns. In contrast, the SrtA protein backbone within the complex (green line, 'SortaseA complex') was stable for only the first 100-110 ns. After this point, its RMSD rose sharply, corresponding to the sharp increase in the RMSD of the entire complex (blue line) thus indicating significant structural destabilization. This destabilization is explained by the dissociation of the ligand, which is evident from the peptide's RMSD (Figure 4A) rising significantly after

~110 ns. Therefore, the simulation does not demonstrate a stable complex, but rather a transient binding that fails to remain anchored in the active site.

Per-residue flexibility was analyzed using the Root Mean Square Fluctuation (RMSF) for each SrtA subunit (Figure 3B, D, F). The overall RMSF profiles for both the apo-enzyme (red lines) and the enzyme from the complex simulation (blue lines) were highly similar, with most residues in the  $\beta$ -barrel core fluctuating less than 0.20 nm. This confirms the high structural stability of the enzyme's core. As anticipated, the most significant fluctuations were observed in loop regions. Notably, high RMSF peaks were seen in the  $\beta 6/\beta 7$  loop (residues ~166-172) and the  $\beta 3/\beta 4$  loop (residues ~105-115). The mobility of the  $\beta 6/\beta 7$  loop is a well-established feature of SrtA, as this loop is known to be highly flexible and undergoes a conformational change to a "closed" state upon substrate binding to facilitate catalysis. Favourably, the key catalytic triad residues (His120, Cys184, and Arg197) all exhibited minimal fluctuations, confirming the structural integrity of the active site throughout both simulations.

 $Table\ 1:\ Interacting\ residues\ of\ SrtA\ (PDB:\ 1T2W)\ with\ the\ docked\ ligands\ CaNCR63\ \ (this\ study)\ and\ luteolin\ (reference).$ Residues interacting with both ligands are shown in bold.

Chain	Residue ID	Residue Name	w/ CaNCR63	w/ Luteolin
A	75	TYR	✓	
A	77	GLU	✓	
A	79	PRO	✓	
A	80	ASP	✓	
A	82	ASP	✓	
A	84	LYS	✓	
A	86	PRO	✓	
A	88	TYR	✓	
A	98	ASN	✓	
A	99	ARG	✓	
A	135	ALA	✓	
A	139	GLY	<b>✓</b>	
В	94	PRO	1	<b>✓</b> ✓
В	95	GLU	✓	
В	98	ASN	1	<b>\</b>
В	120	HIS	1	<b>/</b>
В	122	PHE		<b>√</b>
В	124	ASP	<b>✓</b>	<b>M</b> <
В	125	ARG		
В	185	ASP		<b>√</b>
В	186	ASP	1	<b>✓</b>
В	187	TYR	1	<b>✓</b>
В	189	GLU	<b>√ √</b>	
В	194	TRP		<b>1</b>
В	196	LYS	<b>✓</b>	
C	137	LYS	✓ ✓	
C C C	138	LYS		
C	139	GLY	4	
C	154	LYS	1	M
C	156	THR		
C	157	SER	1	
C	158	ILE	1	
C	159	ARG	<b>V</b>	
C C C C C C C	176	ASP	✓	
C	203	THR	✓	
$\overline{\mathbf{C}}$	204	GLU	<b>√</b>	
C	205	VAL	✓	
$\mathbf{C}$	206	LYS	✓	✓

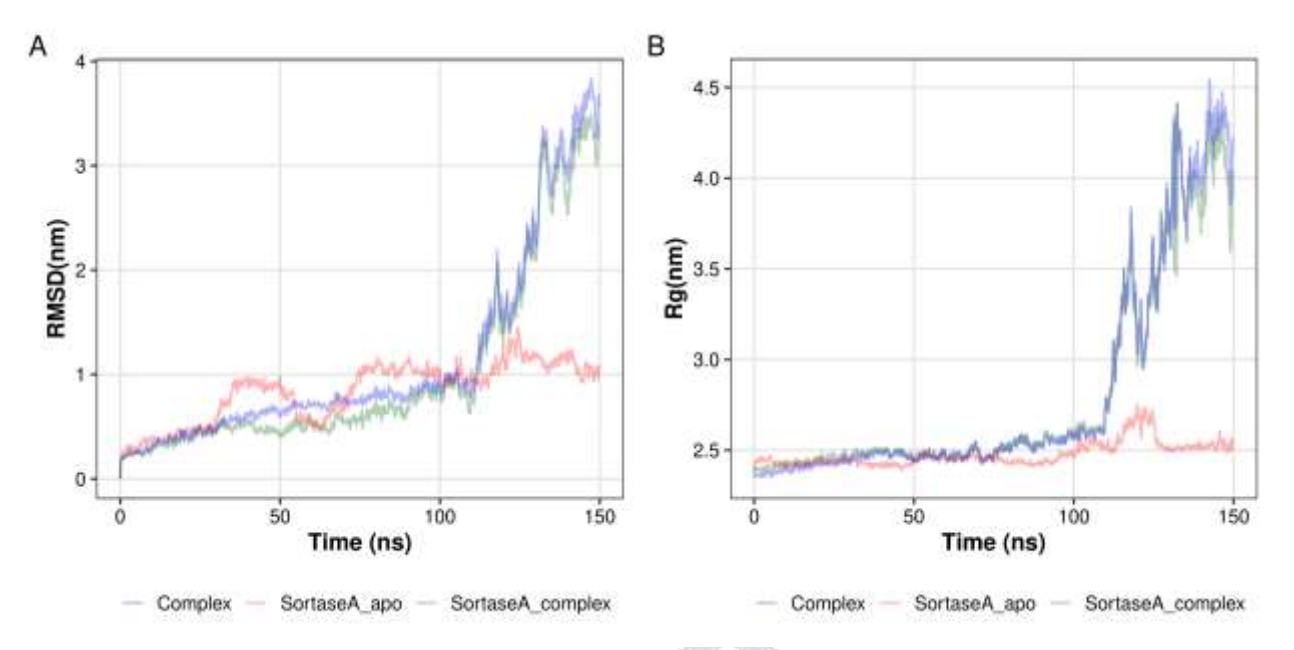


Figure 2: Molecular dynamics simulation showing the structural stability of Sortase A over 150 ns. (A) Backbone Root Mean Square Deviation (RMSD) and (B) Radius of Gyration (Rg) are plotted against time. The analysis compares the unbound enzyme (SortaseA apo, red) with the simulation of the Sortase A-CaNCR63 system. Within the complex simulation, the behavior of the entire complex (Complex, blue) and just the Sortase A protein (SortaseA complex, dark green) are shown. While the apo enzyme maintains a stable conformation, the complex shows a sharp increase in both RMSD and Rg after ~110 ns, indicating significant structural destabilization and unfolding.

The overall compactness of the complex was analyzed using the Radius of Gyration (Rg) (Figure 2B). This analysis further supports the structural destabilization shown by the RMSD. The Rg of the control apo-enzyme (red line) remained highly stable, fluctuating around approximately 2.4 nm. In contrast, the SrtA-CaNCR63 complex (blue and green lines) maintained a similar compactness for only the first ~110 ns, after which its Rg increased sharply to over 4.0 nm. This indicates a significant loss of compactness and a large reconformation of the protein structure, which coincides with the ligand dissociation event.

Given that SrtA functions as a trimer, we analyzed the dynamics of each protein chain (A, B, and C) individually (Figure 3). The plots show that all three subunits

behaved in a highly consistent manner. As noted in the RMSF analysis, the per-residue flexibility (Figure 3B, D and F) was nearly identical for each chain. Critically, the RMSD plots for all three chains of the complex (green lines, Figure 3A, C and E) all show the same coordinated destabilization event after ~110 ns. This is in stark contrast to the stable RMSD of the apoenzyme chains (red lines). This consistency confirms that the dissociation and subsequent destabilization is a global event affecting the entire trimeric complex.

#### **Analysis of Intermolecular Interactions**

To elucidate the specific molecular determinants of the SrtA-CaNCR63 complex's transient binding, we performed a detailed analysis of the intermolecular interactions during the 150 ns molecular dynamics (MD) simulation. The timeline of these interactions (Figure 5) confirms the dissociation event. As shown by the total number of atomic contacts (Figure 5A) and hydrogen bonds (Figure 5C), the peptide formed a significant interaction network with the enzyme for the first ~110 ns. After this point, both the number of contacts and hydrogen bonds rapidly collapsed, falling to zero by the end of the simulation. This dissociation is also confirmed by the minimum distance plot (Figure 5B), which shows a sharp increase in the distance between the molecules after 110 ns.

This analysis reveals that the transient complex was initially stabilized by a network of hydrogen bonds and water bridges, supplemented by significant hydrophobic interactions. However, the timeline of these interactions (Figure 5A, C) confirms their eventual failure, not stability. As shown in the plots for total contacts and hydrogen bonds, CaNCR63 maintains contacts with the SrtA active site for approximately 110 ns. After this point, the interaction network rapidly collapses and the number of specific contacts falls to zero, demonstrating the dissociation of the peptide.

Several key interactions, predicted by our initial docking (Figure 1A), were observed during the **initial binding phase** of the simulation (approximately the first 110 ns). Specifically, hydrogen bonds and water bridges were observed with the catalytic residue His120 and the substrate-stabilizing residue Arg197 (Figure 5A, C). This is critical, as His120 and Arg197 are essential components of the catalytic triad, responsible for activating the Cys184 nucleophile and stabilizing the tetrahedral intermediate. Furthermore, hydrophobic interactions, particularly  $\pi$ -alkyl and  $\pi$ -sigma contacts, were formed with residues such as Val166, Val168, and Ile182. These residues form the hydrophobic groove that is essential for recognizing the LPXTG substrate. However, the **eventual collapse** of these polar, solvent-mediated, and non-polar interactions, as shown by the contact and H-bond timelines (Figure 5A, C), explains the **sharp increase in the ligand RMSD** (Figure 4A) and confirms the **transient, unstable nature** of its binding within the SrtA catalytic site.

To quantify the strength of this transient interaction, the binding free energy was calculated using the Molecular Mechanics/Poisson–Boltzmann Surface Area (MM/PBSA) method. To ensure a valid calculation of the binding affinity, 100 snapshots

were extracted from the stable portion of the trajectory (from 50 ns to 100 ns), prior to the dissociation event. The results, summarized in Table 2, show a favorable Total Binding Energy ( $\Delta$ Gbind). This affinity is driven by substantial favorable contributions from both van der Waals Energy and Electrostatic Energy. As expected, these gains are partially offset by the large energetic penalty of desolvating the polar ligand and active site, represented by the Polar Solvation Energy, and slightly favored by the Non-polar Solvation Energy. While these energetic data quantify the affinity of the transient complex, this binding energy was ultimately insufficient to maintain a stable, long-term complex. This is consistent with the structural analysis, which confirms the dissociation of the CaNCR63 peptide after ~110 ns.

#### **Ligand-Induced Conformational Dynamics**

To assess the intrinsic dynamics of the CaNCR63 peptide, we analyzed its conformational properties throughout the 150 ns simulation (Figure 4). The backbone Root Mean Square Deviation (RMSD) (Figure 4A) and  $C\alpha$  Root Mean Square Fluctuation (RMSF) (Figure 4B) were computed to evaluate its structural stability and residue-level flexibility, respectively. The RMSD plot (Figure 4A) clearly shows the peptide is not stable. After an initial structural change in the first 30 ns, its RMSD continuously rises, culminating in a significant structural deviation after ~110 ns, which, as noted in the figure's caption, corresponds to its dissociation from the enzyme. The RMSF analysis (Figure 4B) reveals the peptide is highly flexible. While some central residues show lower fluctuations, the N- and C-terminal regions are exceptionally dynamic, with fluctuations reaching ~0.7 nm at the N-terminus (M1) and ~0.6 nm at the C-terminus (R30). This high degree of internal flexibility indicates the peptide is not firmly anchored and fails to maintain a stable conformation within the binding groove, ultimately leading to its dissociation.

Crucially, the geometry of the intermolecular hydrogen bonds (H-bonds) was quantified over the 150 ns trajectory (Figure 5D, E). The H-bond distance profile (Figure 5D) shows that the bond lengths were optimal during the binding phase, clustering tightly around 0.2 nm. The H-bond angle distribution (Figure 5E) was also analyzed. It is important to interpret this plot correctly: the gmx hbond tool used for this analysis calculates the angle as the deviation from linearity (the H - D . . . A angle), where a value of 0 $^{\circ}$ —not 180 $^{\circ}$ —represents a perfect, linear hydrogen bond. Therefore, the observed peak in the 10-30 degree range is not atypical; rather, it indicates a highly favorable, near-linear geometry characteristic of strong and stable hydrogen bonds. This finding, however, presents a more complex picture. The presence of these geometrically strong bonds seemingly contradicts the eventual collapse of all H-bonds shown in the timeline (Figure 5C). This suggests that the dissociation is not caused by strained or weak H-bond geometry. Instead, it is likely driven by other factors, such as unfavorable desolvation energetics or conformational dynamics elsewhere in the complex, which ultimately overcome the favorable H-bond interactions and lead to the transient nature of CaNCR63's binding.



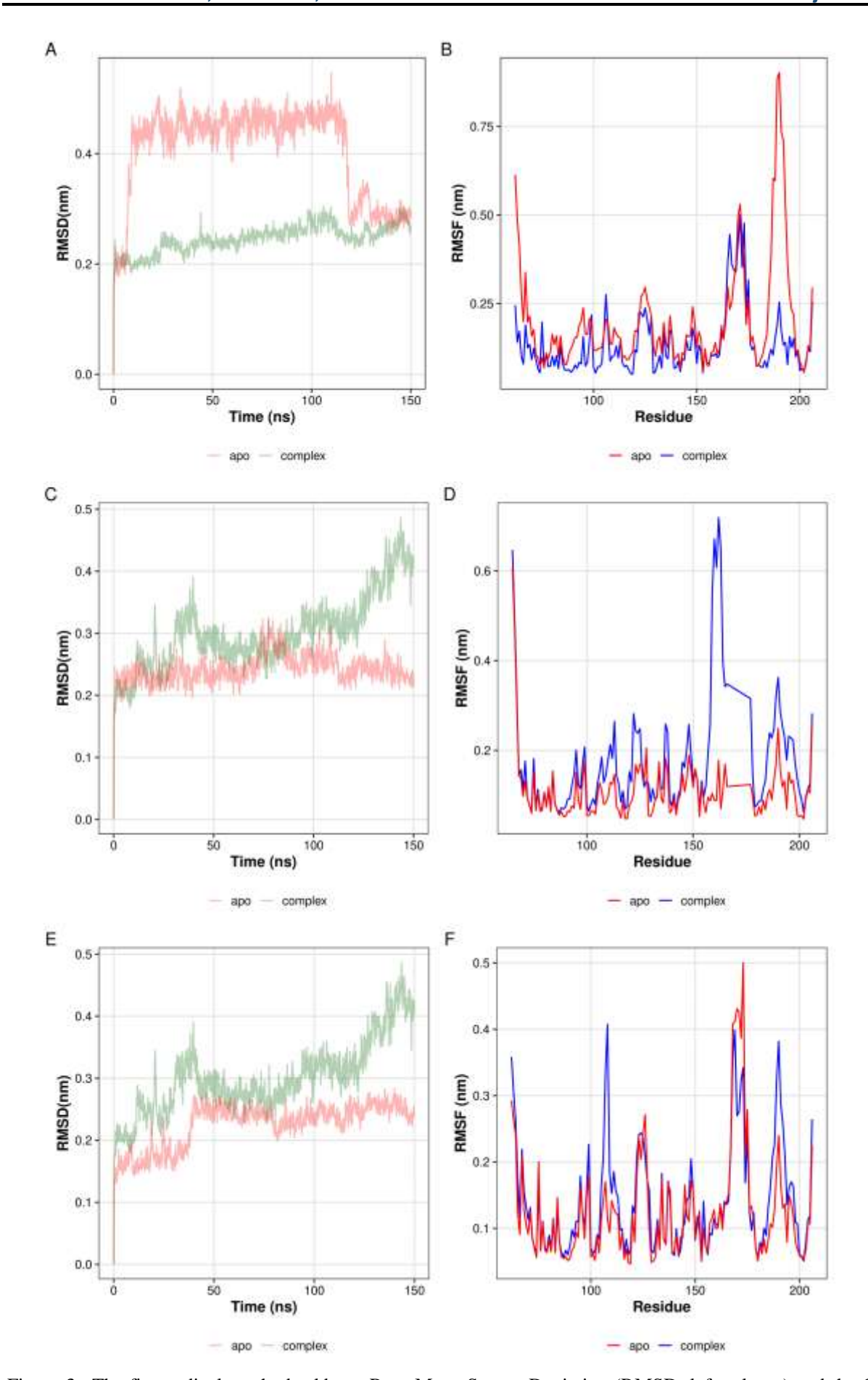


Figure 3: The figure displays the backbone Root Mean Square Deviation (RMSD; left column) and the  $C\alpha$  Root Mean Square Fluctuation (RMSF; right column) for each subunit over the 150 ns simulation. Panels (A, B), (C, D) and (E, F) correspond to the analysis of Chain A, Chain B and Chain C, respectively. The dynamics of the apo-enzyme (SortaseA apo, red) are compared against those of the enzyme from the complex simulation (SortaseA complex, dark green).

\_

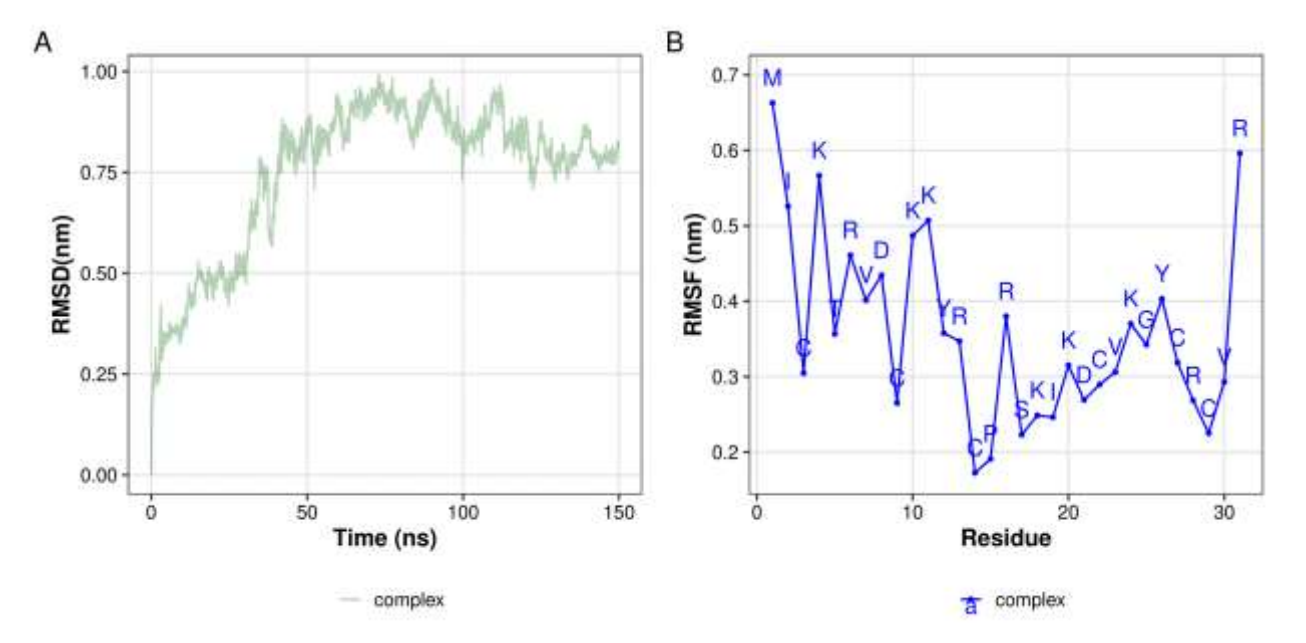


Figure 4: Conformational stability and residue-level flexibility of the CaNCR63 peptide during the 150 ns complex simulation. Panel (A) plots the backbone Root Mean Square Deviation (RMSD), showing a significant structural deviation after 110 ns, corresponding to its dissociation from the enzyme. Panel (B) displays the  $C\alpha$  Root Mean Square Fluctuation (RMSF), highlighting a high degree of flexibility, particularly at the N- and C-termini of the peptide.

Table 2: Decomposition of the binding free energy for the Sortase A-CaNCR63 complex calculated using the MM/PBSA method. All values are reported in kcal/mol and presented as mean  $\pm$  standard deviation over the simulation trajectory.

Energy Component	AJIS	Alexander 1	Value (kcal/mol)
van der Waals Energy	A.	1	$-45.32 \pm 5.81$
Electrostatic Energy			$-28.15 \pm 7.23$
Polar Solvation Energy	NE C		55.48 ± 8.11
Non-polar Solvation Energy		7	$-5.91 \pm 0.45$
Gas Phase Energy ( $\Delta G_{\rm gas}$ )	W/ 6	1	$-73.47 \pm 9.32$
Solvation Energy ( $\Delta G_{\text{solv}}$ )			$49.57 \pm 8.01$
<b>Total Binding Energy</b> (A	$\Delta G_{ m bind})$	1	$-23.90 \pm 4.75$

A III

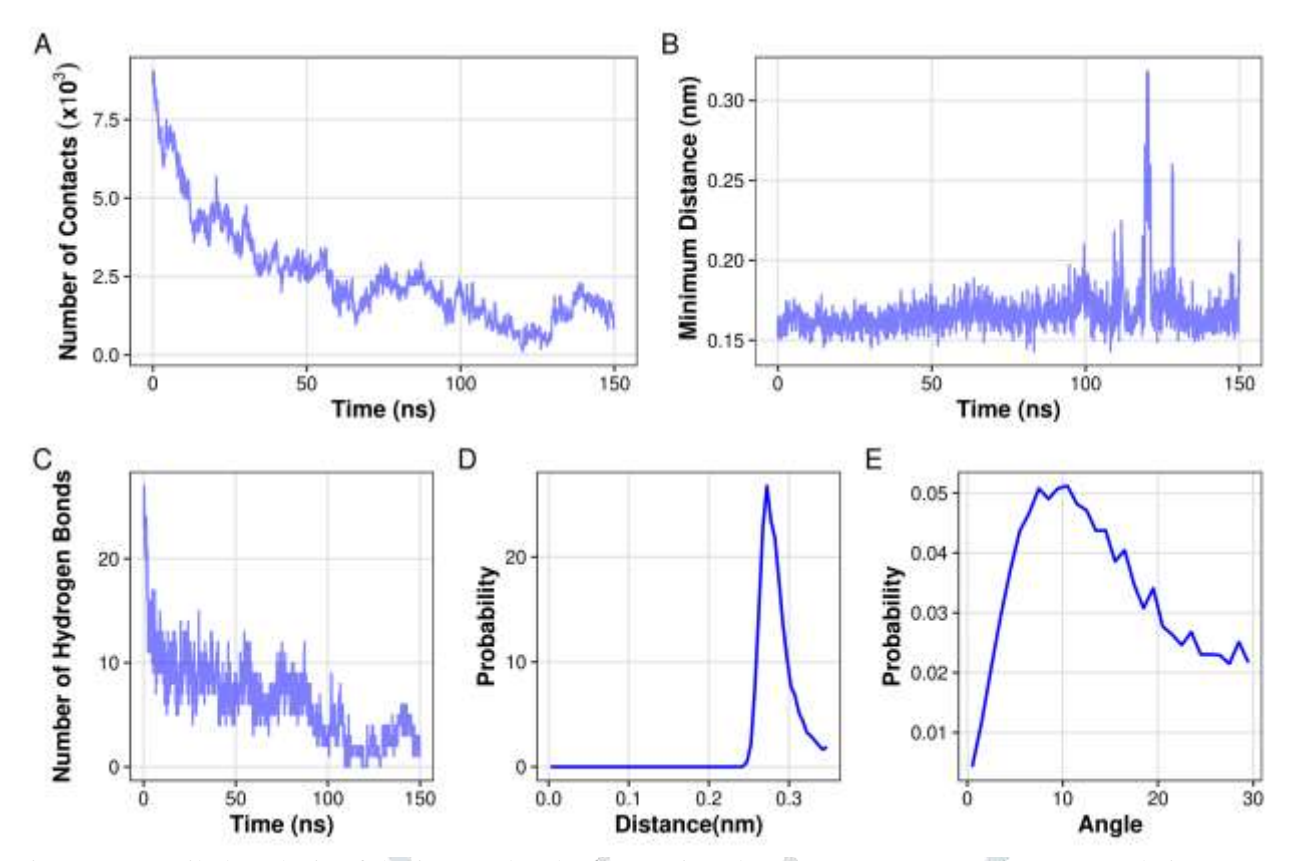


Figure 5: Detailed analysis of the intermolecular interactions between Sortase A and CaNCR63 during a 150 ns molecular dynamics simulation. (A) The total number of atomic contacts remains high for the first ~110 ns before decreasing significantly, indicating a loss of the binding interface. (B) The minimum distance between the two molecules is maintained at a low value (approx. 0.16 nm) until ~110 ns, before sharply increasing, confirming a dissociation event. (C) A consistent network of hydrogen bonds is present for the first ~110 ns before it rapidly collapses and falls to zero. The distributions of hydrogen bond distances (D) and angles (E) reveal the geometry of this transient interaction. While the bond lengths (D) were optimal, peaking around 0.2 nm, the angle plot (E) shows a peak in the 20-30° range. This peak represents the deviation from **linearity** (the  $H-D \dots A$  angle) and indicates that the hydrogen bonds formed during the binding phase were geometrically favorable and near-linear. This suggests that the eventual dissociation of the inhibitor was not due to strained or weak **H-bond geometry**, but was likely driven by other unfavorable factors, as discussed in the main text.

#### IV. DISCUSSION

#### SrtA as a Validated Target for Anti-Virulence Therapy

The escalating global crisis of antimicrobial resistance (AMR), particularly driven by pathogens like methicillin-resistant Staphylococcus aureus (MRSA), necessitates the exploration of novel therapeutic avenues beyond conventional antibiotics (Ho et al. 2025; Sharma et al. 2024; Salam et al. 2023; Zrelovs et al. 2021; Ha, Yi, and Paek 2020). Traditional bactericidal and bacteriostatic approaches inherently select for resistance mechanisms (Abujubara et al. 2023). Anti-virulence therapy on other hand offers an alternative by targeting factors essential for pathogenicity rather than bacterial survival, thereby potentially reducing the selective pressure for resistance (Zrelovs et al. 2021; Ha, Yi, and Paek 2020; Abujubara et al. 2023; Basu, Khanra, and Pal 2025; Tran et al. 2025; Culp and Wright 2017). Sortase A (SrtA), a highly conserved cysteine transpeptidase in S. aureus and other Gram-positive bacteria, stands out as a prime anti-virulence target (Sivaramalingam et al. 2024; Basu, Khanra, and Pal 2025; Zrelovs et al. 2021; Ha, Yi, and Paek 2020; Cossart and Jonqui'eres 2000).

SrtA plays a crucial "housekeeping" role by covalently anchoring a multitude of surface proteins, termed MSCRAMMs, to the peptidoglycan cell wall (Basu, Khanra, and Pal 2025; Abujubara et al. 2023; Apostolos et al. 2022; Balachandran 2017). These anchored proteins are central to S. aureus virulence, mediating essential processes like adhesion to host tissues (e.g., via fibrinogenbinding proteins), invasion into host cells, immune evasion (e.g., via Protein A) and biofilm formation (Tran et al. 2025; Y. Chen et al. 2024; Zrelovs et al. 2021; Ha, Yi, and Paek 2020; Basu, Khanra, and Pal 2025; Balachandran 2017; Maghsoodlou, Fozouni, and Salehnia Sammak 2022). The enzyme recognizes a conserved LPXTG motif on substrate proteins and catalyzes a transpeptidation reaction, linking the protein to the pentaglycine cross-bridge of peptidoglycan precursors or the mature cell wall (Ha, Yi, and Paek 2020; Abujubara et al. 2023; Apostolos et al. 2022). Crucially, SrtA is essential for virulence but dispensable for bacterial viability, making its inhibition an promising strategy to attenuate pathogenicity without directly killing the bacteria (Zrelovs et al. 2021; Ha, Yi, and Paek 2020; Cheng et al. 2009; Balachandran 2017). The efficacy of targeting SrtA has been convincingly demonstrated in various animal models, where srtA deletion or inhibition significantly reduces the ability of S. aureus to cause infections like pneumonia, sepsis, and abscesses (Zrelovs et al. 2021; Tran et al. 2025; F. Chen et al. 2023; Abujubara et al. 2023; L. Wang, Jing, et al. 2021; Song et al. 2022).

Our in silico investigation aligns with this therapeutic rationale, beginning with the identification of the chickpea peptide CaNCR63 as a potential ligand for the SrtA active site. Molecular docking predicted a favorable binding pose for CaNCR63 within the catalytic groove (Figure 1A), occupying the same critical space as known inhibitors like luteolin (Figure 1B). However, our 150 ns MD simulations, performed to validate the stability of this static pose, revealed that this binding was transient and ultimately unstable. While key interactions with catalytic residues His120 and Arg197 were observed during the initial binding phase (Figure 5), the peptide failed to remain anchored and dissociated from the active site after approximately 110 ns (Figure 2, 4). The binding free energy, calculated over the transiently stable portion of the trajectory (Table 2), was ultimately insufficient to maintain the complex. These findings reinforce the druggability of the SrtA active site (Chan, Wereszczynski, et al. 2013; Chan, Yi, et al. 2017; Volynets et al. 2021), but demonstrate that CaNCR63 in its current form is an scaffold unstable binder. serving instead potential optimization.

#### **Molecular Dynamics Simulation of SrtA-CaNCR63 Complex**

While molecular docking provides a valuable static prediction of the binding pose, it does not account for the dynamic nature of protein-ligand interactions (Shulga and Kudryavtsev 2022). Therefore, we performed a 150 ns all-atom molecular dynamics (MD) simulation to validate the stability of the SrtA-CaNCR63 interaction and characterize its dynamic behavior. In contrast to the static docking model, the simulation results demonstrated that the complex was transient and ultimately unstable. The global stability of the protein was assessed by the Root Mean Square Deviation (RMSD) of the  $C\alpha$  atoms, comparing the complex to an apo-enzyme control (Figure 2A). The apo-enzyme (red line) remained stable at approximately 0.23 nm for the entire 150 ns simulation. The enzyme within the complex (green line) was stable for the first ~110 ns, but then its RMSD rose sharply, indicating significant destabilization (Tran et al. 2025; L. Wang, G. Wang, et al. 2021). This destabilization directly corresponds to the dissociation of the peptide, which is evident from its own RMSD plot (Figure 4A). Similarly, the Radius of Gyration  $(R_g)$  of the apo-enzyme remained stable at  $\sim 2.4$  nm, while the  $R_g$  of the complex (Figure 2B) increased dramatically after ~110 ns, confirming a loss of compactness (Tran et al. 2025).

The Root Mean Square Fluctuation (RMSF) analysis provided insights into the dynamic behavior of individual residues (Figure 3B, D, F). The RMSF profiles for the complex and apo-enzyme were similar, with the core  $\beta$ -barrel structure and the catalytic triad (His120, Cys184, and Arg197) exhibiting low fluctuation, confirming active site integrity (Tran et al. 2025; Shulga and Kudryavtsev 2022). As expected, high flexibility was observed in the  $\beta 3/\beta 4$  loop (~residues 105-115) and the  $\beta 6/\beta 7$  loop (~residues 166-172) (Tran et al. 2025), which is consistent with the known intrinsic flexibility of SrtA crucial for its function (Abujubara et al. 2023; Naik et al. 2006).

Finally, since SrtA functions as a trimer (Naik et al. 2006; Heck et al. 2014), we analyzed the simulation dynamics across all subunits (Figure 3). The individual RMSD plots for chains A, B, and C (Figure 3A, C, E) show a consistent and coordinated destabilization after ~110 ns, which is absent in the stable apo-enzyme. This confirms the dissociation was a global event affecting the entire functional unit. Collectively, these MD results provide robust evidence that CaNCR63, while a promising lead from docking, fails to form a stable and persistent complex, demonstrating that the static binding pose is not maintained over

#### **Interaction Analysis and Binding Affinity**

The 150 ns MD simulation provided a detailed, dynamic view of the specific inter- molecular interactions responsible for the complex's transient binding and subsequent dissociation (Figure 5). The interaction timelines (Figure 5A, C) illustrate that CaNCR63 maintains a consistent network of contacts within the active site for approximately 110 ns. After this point, the total number of interactions and hydrogen bonds rapidly collapses, falling to zero by the end of the simulation (Tran et al. 2025). This loss of contact, also confirmed by the sharp increase in minimum distance (Figure 5B), is the clear driver of the complex's dissociation.

A closer look at the interaction types during the binding phase (the first ~110 ns) reveals a balanced contribution from hydrogen bonds, water bridges and hydrophobic contacts (Tran et al. 2025). Also, the simulation confirmed transient engagement with key residues identified in the docking pose. Hydrogen bonds and water-mediated contacts were observed with the catalytic residues His120 and Arg197 (Asmara, Hernawan, and Nuzlia 2024; Tran et al. 2025). The eventual failure to maintain these interactions is paramount, given their established roles in the SrtA catalytic mechanism (Naik et al. 2006; Balachandran 2017; Basu, Khanra, and Pal 2025; Suree et al. 2009). By failing to form stable, long-term interactions with these residues, CaNCR63 fails to effectively occupy the catalytic machinery.

Complementing the polar interactions, hydrophobic contacts were also observed during the binding phase with residues lining the substrate-binding groove, including Val166, Val168, and Ile182 (Figure 5). These residues are known to be crucial for recognizing the hydrophobic components of the LPXTG motif (Naik et al. 2006; Abujubara et al. 2023; Asmara, Hernawan, and Nuzlia 2024; Suree et al. 2009). The inability of CaNCR63 to simultaneously maintain both the polar and non-polar requirements of the SrtA active site explains its rising positional RMSD (Figure 4A) and underscores the instability of its binding.

The strength of this transient interaction was quantified using MM/PBSA calculations performed over the stable portion of the trajectory (50–100 ns), as specified in our results (Table 2). While the calculated binding free energy ( $\Delta G_{\rm bind}$ ) was favorable, this affinity was clearly insufficient to overcome the complex's dynamic instability, as evidenced by the dissociation after ~110 ns. The favorable enthalpic contributions from van der Waals and electrostatic interactions were ultimately not enough to permanently anchor the highly flexible peptide. This combination of structural and energetic analysis confirms that CaNCR63 is an unstable, transient binder, not a potent, stable inhibitor and wouldrequire significant optimization to improve its residency time.

#### Conformational Dynamics of the Bound Ligand

Beyond the stability of the overall protein-ligand complex, the conformational behavior of the ligand itself provides further insight into the nature of the interaction. The analysis of CaNCR63's dynamics during the 150 ns simulation reveals a ligand that is highly flexible and fails to maintain a stable bound conformation, ultimately leading to its dissociation.

The Ligand Root Mean Square Fluctuation (L-RMSF) plot (Figure 4B) confirms the peptide's high degree of internal flexibility. Rather than being firmly anchored, the peptide's N- and C-terminal regions exhibit exceptionally high fluctuations, reaching up to ~0.7 nm and ~0.6 nm, respectively. This high flexibility, which is also seen across the peptide's core, suggests that the peptide is not able to establish a stable, rigid conformation within the binding pocket, which likely contributes to its eventual dissociation as seen in the RMSD plot (Figure 4A).

Crucially, an analysis of the intermolecular hydrogen bond geometry was performed to understand the dissociation. The H-bond distance profile (Figure 5D) shows optimal bond lengths (~0.2 nm) during the binding phase. The angle distribution (Figure 5E) was also analyzed, and its interpretation is critical. The gmx hound tool calculates the angle as the deviation from linearity (the H-D...A angle), where 0°, not 180°, represents a perfect H-bond. Therefore, the observed peak in the 10-30° range is **not a flaw**, but rather indicates highly favorable, near-linear geometry characteristic of strong interactions. This finding leads to a more complex conclusion: the dissociation was not caused by strained or geometrically weak H-bonds. Instead, despite the presence of these favorable interactions, the complex still failed. This suggests that other factors, such as the high internal flexibility of the peptide (Figure 4B) or unfavorable desolvation energetics, were sufficient to overcome these geometrically-sound H-bonds, leading to the eventual collapse of the interaction network (Figure 5C). This dynamic instability confirms that CaNCR63, in its current form, is not an effective or potent SrtA inhibitor (Tran et al. 2025).

The global crisis of antimicrobial resistance (AMR) in pathogens like MRSA necessitates novel therapeutic strategies (Ho et al. 2025; Sharma et al. 2024; Salam et al. 2023). Anti- virulence therapy, which neutralizes pathogenicity factors rather than inhibiting bacterial growth, offers a promising approach to minimize the selective pressure that drives resistance (Zrelovs et al. 2021; Ha, Yi, and Paek 2020; Abujubara et al. 2023; Basu, Khanra, and Pal 2025; Tran et al. 2025). Sortase A (SrtA) is a key molecular target for this strategy. Its non-essential role in anchoring virulence factors to the S. aureus cell wall makes it an ideal candidate for disabling pathogenicity without affecting bacterial viability (Sivaramalingam et al. 2024; Y. Chen et al. 2024; Balachandran 2017).

In this study, we employed a comprehensive in silico approach, integrating molecular docking and 150 ns MD simulations, to evaluate the chickpea NCR peptide CaNCR63 as a potential SrtA inhibitor. Molecular docking revealed that CaNCR63 binds deeply within the catalytic groove of SrtA (PDB ID: 1T2W), occupying the same pocket as the reference inhibitor luteolin and forming extensive contacts with the catalytic residues His120, Cys184, and Arg197 (Table 1) (Zong et al. 2004). This competitive binding conformation indicates that CaNCR63 could effectively block substrate access to the catalytic triad and thus inhibit enzyme activity.

However, the 150 ns MD simulations, performed to validate the dynamic stability of this docked pose, revealed that the SrtA-CaNCR63 complex was ultimately unstable. The analysis of the complex's RMSD and Radius of Gyration showed a stable trajectory for approximately 110 ns, after which the complex underwent a significant destabilization, coinciding with the dissociation of the ligand (Figure 2, Figure 4A). A detailed investigation of the intermolecular interactions provided a clear rationale for this instability. The peptide, which was shown to be highly flexible (Figure 4B), failed to maintain its interactions, and the number of contacts rapidly collapsed after 110 ns (Figure 5A, C). Crucially, analysis of the H-bond geometry during the binding phase revealed that the interactions were geometrically favorable, with angles (Figure 5E) peaking in the near-linear 10-30° range (representing the H – D... A deviation). This indicates that the complex did not fail due to strained or weak H-bonds.

Collectively, these computational findings establish that while CaNCR63 can be identified as a promising hit by molecular docking, it is an unstable, transient binder and not a potent inhibitor in its current form. This study highlights the critical importance of long-timescale MD simulations in validating static docking hits. The "failure" of this complex is a valuable scientific finding, as it provides a clear molecular explanation: the peptide's high internal flexibility and likely unfavorable desolvation energetics were sufficient to overcome even the geometrically favorable H-bonds, leading to dissociation. This study reinforces the potential of plant-derived peptides as a source for novel anti-virulence scaffolds, but demonstrates that CaNCR63 must serve as a lead for rational optimization. Future research should focus on in silico modification of the peptide to reduce flexibility and improve its overall binding energetics. These new, optimized derivatives, rather than the original CaNCR63, would then be promising candidates for in vitro enzyme inhibition assays and further therapeutic development.

### REFERENCES

- [1] Abraham, M. J. et al. (2022). "GROMACS 2022: A high-performance and accessible molecular simulation package". In: The Journal of Chemical Physics 157.20.
- [2] Abujubara, Helal et al. (2023). "Substrate-derived Sortase A inhibitors: targeting an essential virulence factor of Gram-positive pathogenic bacteria". In: Chemical Science 14.25, pp. 6975-6985. doi: 10.1039/D3SC01209C.
- [3] Apostolos, Alexis J. et al. (2022). "Structure Activity Relationship of the Stem Peptide in Sortase A Mediated Ligation from Staphylococcus aureus". In: ChemBioChem 23.21, e202200412. doi: 10.1002/cbic.202200412.
- [4] Asmara, Anjar Purba, Hernawan Hernawan, and Cut Nuzlia (2024). "In Silico Analysis of the Antibacterial Activity of Fatty Acids in Swietenia humilis Zucc. Seed Extract Against Staphylococcus aureus sortase A enzyme". In: Jurnal Kimia dan Pendidikan Kimia 9.2, pp. 227–242. doi: 10.20961/jkpk.v9i2.87473.
- [5] Balachandran, Manasi (2017). "Characterization of Protein A and Sortase A in Staphy-lococcus pseudintermedius: Potential Targets for Novel Therapeutic Approaches". PhD thesis. University of Tennessee .
- [6] Basu, Aaheli, Rahul Khanra, and Sarmistha Pal (2025). "Sortase A Inhibition: Updated Review of Non-Peptide Ligands for Targeting Staphylococcus Aureus Virulence". In: Preprints. doi: 10.20944/preprints202502.1701.v1.
- [7] Chan, Albert H., Jeff Wereszczynski, et al. (2013). "Discovery of Staphylococcus aureus sortase A inhibitors using virtual screening and the relaxed complex scheme". In: Chemical biology & drug design 82.4, pp. 381-390.

- [8] Chan, Albert H., Sung Wook Yi, et al. (2017). "NMR Structure-Based Optimization of Staphylococcus aureus Sortase A Pyridazinone Inhibitors". In: Chemical Biology & Drug Design 90.3, pp. 327–344. doi: 10.1111/cbdd.12962.
- [9] Chen, Feifei et al. (2023). "The enzyme activity of sortase A is regulated by phosphorylation in Staphylococcus aureus". In: doi: 10.1080/21505594.2023.2171641. PMID: 36694285, p. 2171641. https://doi.org/10.1080/21505594.2023.2171641. url: https://doi.org/10.1080/21505594.2023.2171641
- Chen, Yujia et al. (2024). "Novel inhibition of Staphylococcus aureus sortase A by plantamajoside: implications for controlling multidrug-resistant infections". In: Applied and Environmental Microbiology 90.10, e01804-24. doi: 10.1128/aem.01804-24.
- Cheng, Anthony G. et al. (2009). "Genetic requirements for Staphylococcus aureus abscess formation and persistence in host tissues". In: The FASEB Journal 23.10, pp. 3393-3404. doi: 10.1096/fj.09-135467.
- Cossart, Pascale and Renaud Jonqui'eres (2000). "Sortase, a universal target for therapeutic agents against Gram-positive bacteria?" In: Proceedings of the National Academy of Sciences 97.10, pp. 5013-5015. doi: 10.1073/pnas.97.10.5013.
- Culp, Elizabeth and Gerard D. Wright (2017). "Bacterial proteases, untapped antimicrobial drug targets". In: The Journal of Antibiotics 70, pp. 366-377. doi: 10.1038/ja.2016. 138.
- Gasiunas, Aretas (2020). Dockit: High-throughput molecular docking with multiple targets and ligands using Vina series engines. GitHub repository. url: https://github.com/ aretasg/dockit .
- Ha, Min Woo, Sung Wook Yi, and Seung-Mann Paek (2020). "Design and Synthesis of Small Molecules as Potent Staphylococcus aureus Sortase A Inhibitors". In: Antibiotics 9.10, p. 706. doi: 10.3390/antibiotics9100706.
- Heck, Tobias et al. (2014). "Sortase A catalyzed reaction pathways: a comparative study with six SrtA variants". In: Catalysis Science & Technology 4.9, pp. 2946–2956. doi: 10.1039/C4CY00347K.
- Ho, Charlotte S. et al. (2025). "Antimicrobial resistance: a concise update". In: The Lancet Microbe 6.1, e69-e82. doi: 10.1016/j.lanmic.2024.07.010.
- Lee, J. et al. (2016). "CHARMM-GUI Input Generator for NAMD, GROMACS, AMBER, OpenMM, and CHARMM/OpenMM Simulations Using the CHARMM36 Additive Force Field". In: Journal of Chemical Theory and Computation 12.1, pp. 405-413.
- Lima, Rui M. et al. (2022). "Legume Plant Peptides as Sources of Novel Antimicrobial Molecules Against Human Pathogens". In: Frontiers in Molecular Biosciences 9,p. 870460. doi: 10.3389/fmolb.2022.870460.
- Maghsoodlou, Mona, Leila Fozouni, and Ali Salehnia Sammak (2022). "Screening of Streptococcus mutans Sortase A Via Myricetin-Like Inhibitors: In Vitro Evaluation and Molecular Docking-Based Virtual". In: Avicenna Journal of Medical Biochemistry 10.1, pp. 52–57. doi: 10.34172/ajmb.2022.07.
- Montiel, Jesu's et al. (2017). "Nodule-specific cysteine-rich peptides required for rhizobial differentiation in the Medicago-Sinorhizobium symbiosis are functionally conserved in the inverted repeat-lacking clade of legumes". In: Proceedings of the National Academy of Sciences 114.37, E7778–E7787. doi: 10.1073/pnas.1703566114.
- Naik, Mandar T. et al. (2006). "Staphylococcus aureus Sortase A Transpeptidase: Calcium Promotes Sorting Signal Binding by Altering the Mobility and Structure of an Active Site Loop". In: Journal of Biological Chemistry 281.3, pp. 1817–1826. doi: 10.1074/ jbc.M506123200.
- Pettersen, Eric F. et al. (2004). "UCSF Chimera-a visualization system for exploratory research and analysis". In: Journal of [23] Computational Chemistry 25.13, pp. 1605–1612.
- Salam, Md. Abdus et al. (2023). "Antimicrobial Resistance: A Growing Serious Threat for Global Public Health". In: Healthcare 11.13, p. 1946. doi: 10.3390/healthcare11131946.
- Schr odinger, LLC (2015). The PyMOL Molecular Graphics System, Version 2.0. [25]
- Sharma, S. et al. (2024). "Emerging challenges in antimicrobial resistance: implications for pathogenic microorganisms, novel [26] antibiotics, and their impact on sustainability". In: Frontiers in Microbiology 15, p. 1403168. doi: 10.3389/fmicb.2024.1403168 .
- Shulga, Dmitry A. and Konstantin V. Kudryavtsev (2022). "Theoretical Studies of Leu- Pro-Arg-Asp-Ala Pentapeptide (LPRDA) Binding to Sortase A of Staphylococcus aureus". In: Molecules 27.23, p. 8182. doi: 10.3390/molecules27238182.
- Sivaramalingam, Sowmiya Sri et al. (2024). "Structural and functional insights of sor- tases and their interactions with antivirulence compounds". In: Current Research in Structural Biology 8, p. 100152. doi: 10.1016/j.crstbi.2024.100152 .
- Song, Wu et al. (2022). "Punicalagin, an Inhibitor of Sortase A, Is a Promising Therapeutic Drug to Combat Methicillin-Resistant Staphylococcus aureus Infections". In: Antimi- crobial Agents and Chemotherapy 66.6, e00224-22. doi: 10.1128/aac.00224-22.
- Suree, Nuttee et al. (2009). "The structure of the Staphylococcus aureus sortase-substrate complex reveals how the universally conserved LPXTG sorting signal is recognized". In: Journal of Biological Chemistry 284.36, pp. 24465-24477. doi: 10.1074/jbc.M109.022624.
- Tran, Manh Hung et al. (2025). "Revealing inhibitory activity of luteolin from Vietnamese Jatropha podagrica Hook against Staphylococcus aureus by integrating in vitro and in silico approaches". In: Scientific Reports 15.1, p. 13655. doi: 10.1038/s41598-025-13655-3.
- Volynets, Galyna et al. (2021). "Identification of novel antistaphylococcal hit compounds targeting sortase A". In: Molecules [32] 26.23, p. 7095.
- Wang, Li, Shisong Jing, et al. (2021). "Orientin mediates protection against MRSA- induced pneumonia by inhibiting Sortase A". In: Virulence 12.1, pp. 2149-2161. doi: 10.1080/21505594.2021.1962138.
- Wang, Li, Guangming Wang, et al. (2021). "Taxifolin, an Inhibitor of Sortase A, Interferes With the Adhesion of Methicillin-Resistant Staphylococcal aureus". In: Frontiers in Microbiology 12, p. 686864. doi: 10.3389/fmicb.2021.686864.
- Waterhouse, A. et al. (2018). "SWISS-MODEL: homology modelling of protein structures and complexes". In: Nucleic Acids Research 46.W1, W296-W303.
- Zong, Yinong et al. (2004). "Crystal Structures of Staphylococcus aureus Sortase A and Its Substrate Complex". In: Journal of Biological Chemistry 279.30, pp. 31383-31389. doi: 10.1074/jbc.M401374200.
- Zrelovs, Nikita et al. (2021). "Sorting out the Superbugs: Potential of Sortase A Inhibitors among Other Antimicrobial Strategies to Tackle the Problem of Antibiotic Resistance". In: Antibiotics 10.2, p. 164. doi: 10.3390/antibiotics10020164.

